Statistical Evidence for a Frequency Dependent Flux Limit of Solar Radio Bursts in the GHz Range

Gelu M. Nita, Louis J. Lanzerotti and Dale E. Gary

Center for Solar -Terrestrial Research

New Jersey Institute of Technology

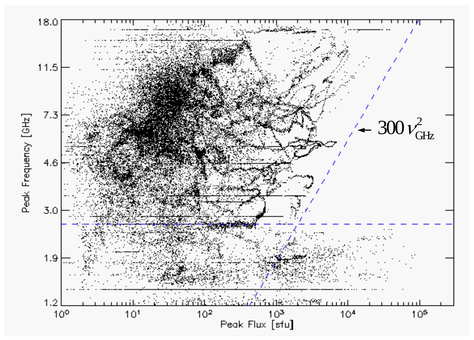

Figure 1 – Synopsis of 2001-2002 OVSA data: The distribution of spectral peak at each recorded instant of time for 412 analyzed events, (500 spectral components, 50733 data points). The horizontal dashed line at 2.6 GHz represents the empirical dividing line between decimetric and centimetric radio emission. The inclined dashed line approximately marks the frequency-squared peak-flux limit revealed by this dataset.

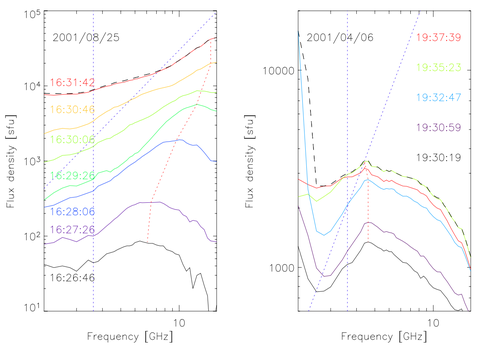

Figure 2 – Evolution of two bursts from the OVSA dataset. The red dashed lines represent the evolution of the spectral peaks, which do not cross the empirical limits set by the blue dashed lines defined in Fig. 1. The black dashed lines represent the envelope of maximum flux recorded at each frequency. It is seen that a particular burst may evolve in such a way that the maximum flux envelope may cross the spectral peak limit, although the spectral peak does not cross it. The maximum flux envelopes are represented, for the whole dataset, in Fig. 3.

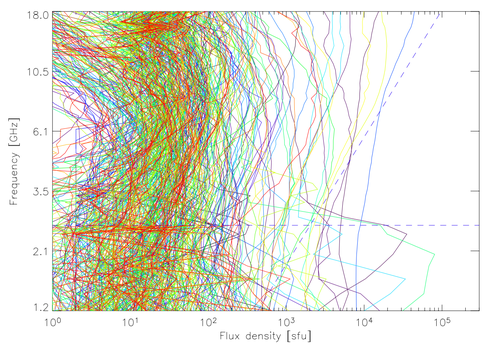

Figure 3 – The maximum flux envelopes for the 2001-2002 OVSA dataset. The blue dashed lines represent the empirical limits found for the spectral peak evolution of the microwave bursts recorded by OVSA. It may be seen that, while most of the bursts did not exceed the spectral peak limits at any frequency during the burst evolution, 11 of the most intense radio bursts crossed these limits (although their instantaneous spectral peaks, as shown in Fig. 1 and 2, evolved inside these boundaries).

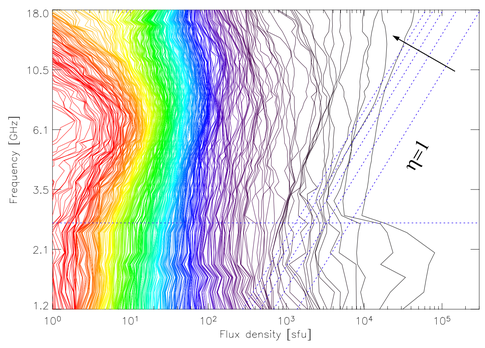

Figure 4 – Contour plot of the flux levels reached or exceeded by a given number of bursts at any of the observed frequencies. The contour levels differ by one count, ranging from 1 (right-black) to 412 (left-red). The Level-1 contour represents the highest flux levels recorded at any OVSA frequency during 2001 and 2002.

The inclined blue dashed lines represent the thermal noise levels in a receiving antenna given by Eq. 1, for η=1, 1/2, 1/3, 1/4 and 1/5, respectively. The arrow indicates the direction in which η decreases. The horizontal blue dashed line at 2.6 GHz represents the empirical dividing line between decimetric and centimetric radio emission.

It is seen that a receiving antenna operating just above the 2.6 GHz limit has little probability to be affected by a high flux radio bursts when operating above the η=1 noise level, but it has an increased probability when η decreases. However, the probability of an interfering radio burst may be kept low when η decreases by increasing the operating frequency.

Introduction

A recent study by Nita, Gary and Lee (2004) has examined a two year set of radio burst spectra that were obtained at the Owens Valley Solar Array (OVSA). These data, obtained during the maximum period of solar cycle 23, are ideal for examining the statistics of solar radio burst amplitudes as a function of frequency in the GHz band of most interest for many contemporary radio receiving systems (e.g., wireless, radar). We demonstrate in this study that, statistically, there is indeed, as suggested before by Nita et. al (2002), a possible preferred frequency range (in the lower GHz band) for reduced solar radio burst flux from a given event. We show the results from these data and discuss their implications for radio system design and operations.

Description of Data

This study is based on a dataset containing all burst total-power spectra recorded by OVSA during 2001 and 2002. Each individual spectrum has been carefully calibrated and the averaged pre-burst spectrum has been subtracted. Each significant spectral component has been identified and its spectral and temporal dynamics has been investigated. **Table 1** presents some statistical information about this dataset.

Table 1– Statistics of OVSA dataset

Year	Events	Spectral Components (1, 2, 3 or more)	Temporal Peaks (1, 2, 3 or more)	Snapshots
2001	**228**	**285** (76.8 %, 21.5 %, 1.7 %)	**672** (38.2%, 25.4%, 36.4%)	**29,682**
2002	**184**	**215** (83.2 %, 16.8 %, 0.0 %)	**450** (40.8 %, 25.0 %, 34.2%)	**21,051**
Total	**412**	**500** (79.6 %, 19.4 %, 1.0 %)	**1,122** (39.3 %, 25.2 %, 35.5%)	**50,733**

Frequency-Dependent Peak Flux Limit of Microwave Bursts

The spectral peak evolution of each spectral component identified in the 2001-2002 OVSA dataset is displayed in **Figure 1**, reproduced from Nita, Gary and Lee (2004) . Two radio burst populations are revealed. The superposition of these two populations, one limited in frequency and the other in intensity, results in a well delimited region in which no high intensity spectral peak can be observed. A similar result was reported by Nita et al. (2002) who, analyzing a 40 year radio burst dataset compiled by NOAA, noticed a lack of events peaking above 1000 sfu at intermediate centimetric wavelengths. This finding may be of particular importance in the context of radio receiving systems, since a gap in solar radio noise level is suggested in the radio frequency band of most interest for the contemporary devices. However, from this perspective, one should be aware that the spectral peak limit does not necessarily imply a limit of radio emission in the same frequency range at any time during the burst evolution. **Figure 2** indicates that a more appropriate magnitude to be monitored in relation with radio burst interference likelihood is the maximum flux envelope of each bursts, defined by the maximum flux recorded at each frequency at any time during the burst evolution.

Maximum Flux Distribution of Microwave Bursts

The frequency resolution of OVSA, which allows quasi-simultaneous observations of up to 40 frequencies in the [1.2,18] GHz band, offers an unique possibility for monitoring the maximum flux distribution of solar radio bursts. **Figure 3** displays the maximal spectral envelopes of all bursts in the dataset. During two years of observation, only 11 bursts out of 412, (2.67%), displayed flux density levels above the empirical limits found for the spectral peak evolution displayed in **Figure 1**. However, this number represents 64.75% of the 17 bursts exceeding 1000 sfu above 2.6 GHz, which points out the necessity of a more carefully analysis of the maximum flux distribution of large-scale bursts in order to set more accurate limits for the solar radio burst emission in the microwave range. **Figure 4** displays the contour plots of the flux levels reached or exceeded by a given number of bursts at each of the monitored frequencies. The shape of this two dimensional cumulative distribution in the high flux region is of most importance in this study, since such flux levels become comparable with the thermal noise floor in a receiving system,

$$F_{\text{thermal noise}} = 960\eta\nu^2 \text{ (sfu)} \qquad (1)$$

where ν is expressed in GHz and the dimensionless factor $\eta = (T/273K)/(G/10)$ equals unity for a typical receiving system operating at room temperature and having an antenna gain of 10 (Gary et al. 2003).

Power-Law Prediction versus Real Data

Figure 5 displays the one dimensional cumulative distributions, (no data binning involved), at some of the OVSA frequencies, which are all very well fitted by power laws in the range [30-1000] sfu, while significant deviations from these fits are displayed above 1000 sfu. To better understand the significance of these deviations, we compare in **Figure 6** some of the contour levels from Fig. 4 with the corresponding ±3σ contour intervals predicted from the power-law fits. We conclude that the power-law prediction fails to describe the real data, especially inside the angular region defined by the spectral peak limits, where the observed distribution displays a frequency dependent roll-over which cannot be explained in the limit of expected statistical deviations from the power-law fits. We interpret this frequency dependent cut-off in the maximum flux distribution as due to the interplay between the spectral peak limitation of centimetric bursts and the distribution of their optically thick spectral slope. The spectral peak limit has been attributed by Lee, Nita and Gary (2004) to a limitation of the product between radio source area and brightness temperature, while the median value of the optically thick spectral slope of high intensity centimetric bursts is 1.4±0.4, as reported by Nita, Gary and Lee (2004). Another important characteristic of high flux microwave bursts is the enhanced decimetric emission, which has been found by Nita, Gary and Lee (2004) to be present in about 60% of the radio bursts exceeding 1000 sfu in the centimetric range. All these findings result in a typical spectral shape of the high flux bursts which, as illustrated in **Figure 7b,** develops a minimum around 3 GHz responsible for the observed emission gap found in this dataset.

Conclusion

The analysis of the maximum flux envelopes of 412 solar radio bursts recorded by OVSA during 2001-2002 at 40 frequencies in the [1.2-18] GHz frequency range gives rise to the following results:

- There is an increased probability for the radio and radar systems operating below 2.6 GHz to be affected by radio interferences caused by solar radio bursts.
- The drop in solar radio interference probability above about 2.6 GHz is probably due to a frequency dependent flux limit of solar radio bursts, which displays a minimum around 3 GHz.
- During the studied interval of the recent solar maximum, there was little chance of radio interference due to solar activity for any system operating above 2.6 GHz and above a typical thermal noise floor (η=1) as defined in Eq. 1.
- If the radio or radar system is to operate with higher sensitivity relative to the thermal noise floor, then the system operating frequency should be shifted to higher frequencies.
- If solar activity suggested the probability of a solar burst event, radio and radar systems could switch their operations to a less susceptible frequency band above 2.6 GHz.

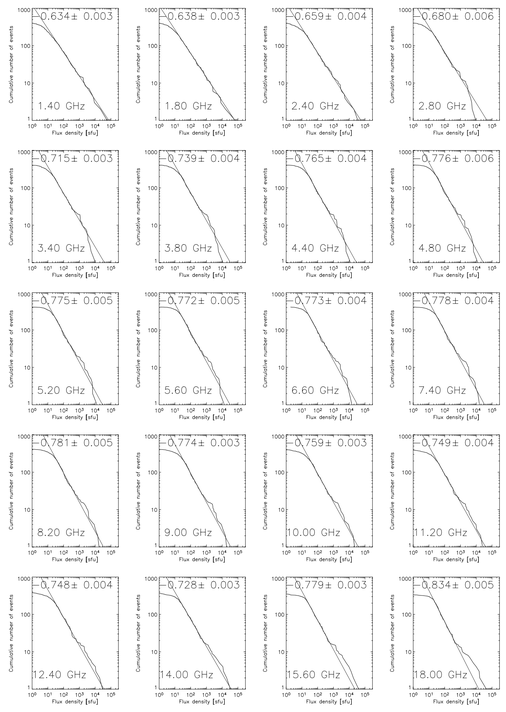

Figure 5 – Cumulative distributions for 20 OVSA frequencies derived from the 2-dimensional distribution represented in Fig. 4. Each distribution is very well fitted by a power-law over the [30-100] sfu range, while noticeable frequency-dependent deviations may be observed above 1000 sfu for the frequencies above 2.6 GHz. The power-law index and its 1-σ standard deviation are indicated on each panel.

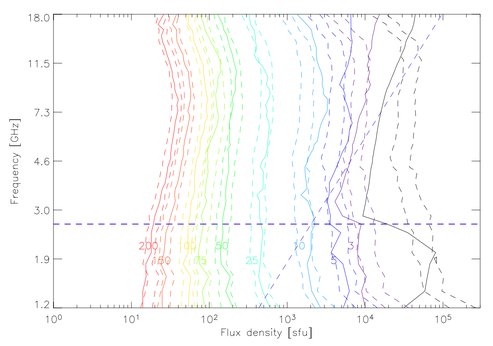

Figure 6 – Data contour plots for 10 different levels (solid lines) and estimated contour levels predicted by the power-law fits as described in Fig. 5. Each pair of dashed lines represents the ±3σ interval predicted for the corresponding data contour indicated by the same color solid line. This figure reveals large deviations of the real data contours above 1000 sfu, which cannot be attributed to statistical fluctuations from the power-law predicted levels. The 1-event power-law contour largely overestimates the corresponding data contour segment bounded by the empirical limits represented in Fig. 1. More or less, the same trend may be observed for all data contours crossing the angular region defined by these two limits.

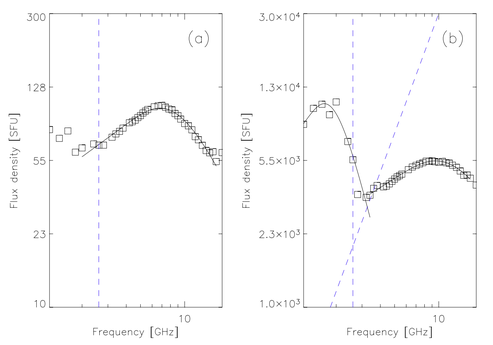

Figure 7 – Averaged spectra of the radio bursts peaking in the centimetric range below, (a), and above, (b), 1000 sfu. The blue dashed lines represent the empirical limits found for the spectral peak evolution. The small-scale radio bursts have a spectral peak below 10 GHz, averaging about 100 sfu. The large-scale radio bursts have one spectral peak in the centimetric range, around 10 GHz, averaging about 5000 sfu, and a more intense spectral peak in the decimetric range, while the less intense radio emission is around 3 GHz. The averaged spectrum of large-scale bursts, which is a typical U-type spectrum as previously defined by Castelli and Guidice (1972), is consistent with the gap of radio emission found in the OVSA dataset.

References:

Statistical Study of Two Years of Solar Flare Radio Spectra Obtained with OVSA
Gelu M. Nita, Dale E. Gary, and Jeongwoo Lee, 2004, ApJ, 605

Nonthermal Electrons in Solar Flares Derived from Microwave Spectra
Jeongwoo Lee, Gelu M. Nita, and Dale E. Gary, 2004, submitted to ApJ

Effects of Solar Radio Bursts on Wireless Systems
Dale E. Gary, Louis J. Lanzerotti, Gelu M. Nita and David J. Thomson, Presented at ESPIRIT, Nato Advanced Research Workshop, 25-29 March 2003, Rhodes, Greece

The Peak Flux Distribution of Solar Radio Bursts
Nita, G. M., Gary, D. E., Lanzerotti, L. J., Thomson, D. J., 2002, ApJ, 570, 423

Acknowledgements:

This work was supported by NSF grants ATM-0077273 and AST-0307670 to the New Jersey Institute of Technology.